Color holographic display based on azo-dye-doped liquid crystal
(Invited Paper)

Xiao Li (李 潇), Chao Ping Chen (陈超平)*, Yan Li (李 燕), Xinhong Jiang (姜新红), Hongjing Li (李洪婧), Wei Hu (胡 伟), Gufeng He (何谷峰), Jiangang Lu (陆建钢), and Yikai Su (苏翼凯)**

National Engineering Lab for TFT-LCD Materials and Technologies, Department of Electronic Engineering, Shanghai Jiao Tong University, Shanghai 200240, China

**Corresponding author: ccp@sjtu.edu.cn; **corresponding author: yikaisu@sjtu.edu.cn*

Received March 10, 2014; accepted March 27, 2014; posted online May 20, 2014

A multiplexed holographic display video has been achieved by using a passive azo-dye-doped liquid crystal (LC) cell. Holograms formed in this cell can be refreshed in the order of several milliseconds. By angular multiplexing technique, dynamically multiplexed holographic videos are realized. Moreover, the reconstructed RGB images are merged into a color image, which illustrates the possibility of a color holographic three-dimensional (3D) display by holographic multiplexing of the LC cell.

OCIS codes: 090.5694, 090.1705.
doi: 10.3788/COL201412.060003.

Three-dimensional (3D) display technologies have attracted worldwide attention and been developed vigorously since the blockbuster movie "Avatar" was released. Usually, 3D displays are classified into two types according to principles of stereopsis. One type is based on binocular disparity with glasses/helmet stereoscopic displays or parallax barriers/lens array[1]. With the development of liquid crystal (LC) displays, these techniques are relatively mature and have become commercial productions. The other type, including holographic display, integral imaging display and volumetric display, is based on 3D scene reconstruction[2−3]. Compared to stereoscopic display of 3D images, these techniques are true 3D displays that provide more depth perceptions. So, the discomfort and fatigue can be avoided effectively. These techniques are currently under active research and lacking in commercial productions. Among these 3D display techniques, holographic display is considered as an ultimate goal to provide realistic image of a real object or scene, because it has the ability to reconstruct both the intensity and wavefront information of light from a nature object, allowing the observer to perceive the light as if it is scattered by the real object itself without the need for a special eyewear. Therefore, many research groups have been studying the holographic displays of real 3D images, including dynamic materials[4−10], holographic backlight used for flat panel[11], and computer-generated holography (CGH)[12], etc. Large-sized static holographic displays, including full-parallax holographic stereograms using special holographic recording materials, and small-sized dynamic holographic displays based on commercially available spatial light modulators, have been realized by some companies and scientific research institutes. However, limited to computing capacity and very large scale integration (VLSI) technology, it is difficult to realize the video-rate image reconstruction using digital holography (DH). In fact, real-time holographic display is an important and challenging problem to solve and a variety of technologies have been developed to address this challenge. Optical purely reconstruction based on the dynamic recording materials might be an effective way for the video-rate holographic display without huge data post-processing.

In this letter, we use LC 5CB doped with Disperse Red 1 to realize the video-rate holographic display. With this cell, holograms can be refreshed in the order of several milliseconds, which is fast enough to enable video application. By angular multiplexing of holograms, a color image is obtained by the superposition of R/G/B sub-images.

The material used in our experiments is a mixture consisting of 96 wt% of nematic LC (5CB, Sigma-Aldrich, USA) and 4 wt% of Disperse Red 1 (DR1, Sigma-Aldrich, USA). A mylar slip with a thickness of about 50 μm is sandwiched between two glass substrates, both of which are rubbed to align the LC director. The mixture was stirred for 24 hours, and then filled into the cell by capillary action at room temperature. Due to the interaction between DR1 and LC molecules, DR1 molecules are bound to LC molecules in the same orientation and the cell exhibits the characteristics of anisotropic absorption. In this cell with a size

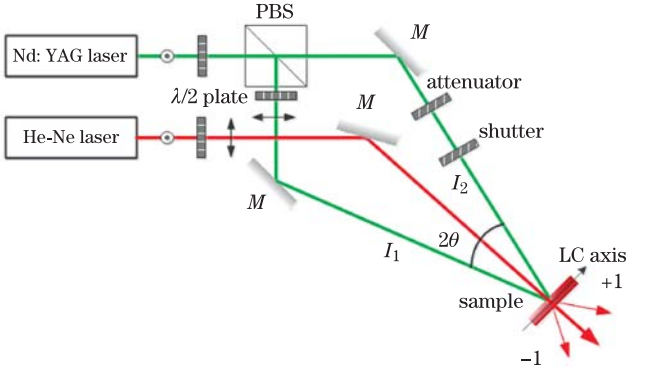

Fig. 1. (Color online) Experimental setup for response time testing with I_1=2.3 mW/mm^2, I_2=2.2 mW/mm^2 and 2θ=21°. M: mirror; BS: beam splitter; $\lambda/2$ plate: half-wave plate.

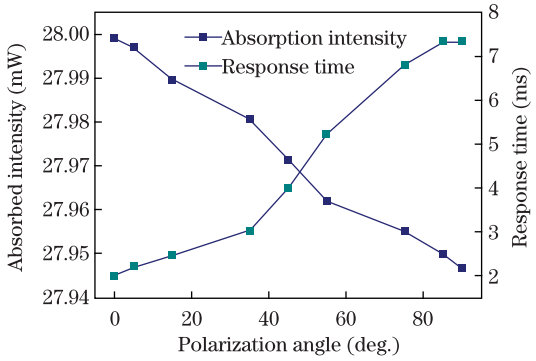

Fig. 2. (Color online) Dependence of anisotropic absorption and response time on the polarization angle.

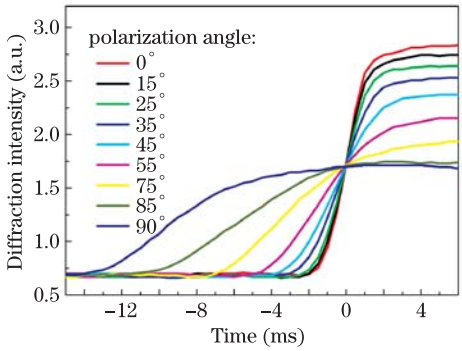

Fig. 3. (Color online) Slopes of grating formation with different angles between the polarization direction of recording light and LC director.

of 2.5× 2.0 (cm), a holographic grating is formed by the interference of two Nd:YAG laser beams, and its dynamic behavior is investigated using the setup shown in Fig. 1. The experimental plane defined by the wave vectors of two recording beams is perpendicular to the substrate of the cell, with the LC director vertical to the experimental plane. Two recording beams emitted from a Nd: YAG laser (λ = 532 nm) are set to be s polarized by a half-wave plate. A beam from the He-Ne laser, which is also s polarized, is used to read the holograms.

We use half-wave plates to change the polarization direction of the recording beams continuously from parallel to perpendicular relative to the director of LC molecules. The dependence of the anisotropic absorption and response time on the recording light polarization are measured by a photodetector, and depicted in Fig. 2. When the LC director is parallel to the beam polarization, which is indicated by the peak anisotropic absorption, the grating is formed in the shortest time. The response curves of the first order diffraction intensity measured at different polarization angles are shown in Fig. 3. The best response time for recording is measured as 1.9 ms.

To achieve a real-time color holographic display, the sample must have the ability to multiplex. Figure 4 illustrates the experimental setup for an angular multiplexed holographic display. A reference beam and an object beam with both diameters about ∼2.5 mm, emitted from a Nd: YAG laser (λ = 532 nm), are set to be p-polarization. Three laser beam expanders are placed along the object beam path. The spatial information of three videos are generated by 3 spatial light modulators (SLMs) respectively. The SLMs, developed by HOLOEYE Photonics AG, are pure phase modulating microdisplays with 1920 × 1080 pixel resolution, 8.0-μm pixel pitch and 60-Hz frame rate. The object beams and reference beams interfere within the sample, which is placed near the Fourier plane of the lenses (F= 400 mm).

By angular multiplexing, three holograms are recorded in the LC cell at the same time. Beams I_1 and I_2 record Hologram D, Beams I_3 and I_4 record Hologram B, Beams I_5 and I_6 record Hologram C. Each reference beam has a light intensity of 2.2 mW/mm^2, and each object beam has a light intensity of 1.6 mW/mm^2. The three holograms are recorded simultaneously, and read out by the red laser. According to multiplexing technique, holographic gratings are recorded at the same spot, these gratings erase mutually, that is, the recording of one hologram also erases other holograms at the same location. In Fig. 5, when I_3 is turned on with the arrow indicating the recording of grating 2, it shows that the diffraction intensity decreases for the first grating and increase for the second grating in several milliseconds. The average diffraction efficiency can be described as Eq. (1)[13],

$$\eta \approx \left(\frac{\pi d \Delta\bar{n}}{\lambda M}\right)^2, \quad (1)$$

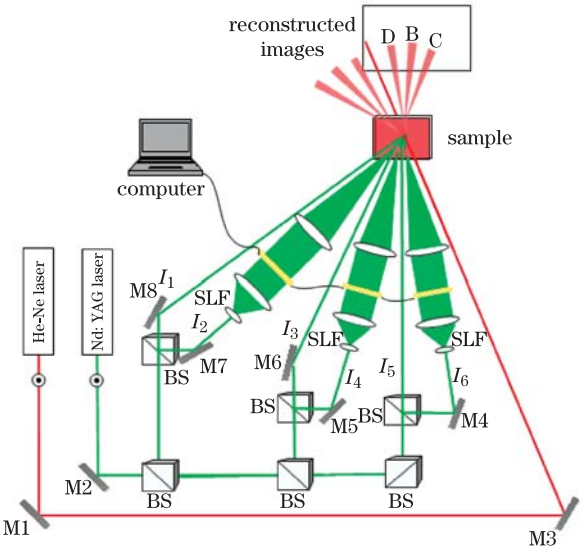

Fig. 4. (Color online) Experimental setup for tri-multiplexed holograhic display. M: mirror; BS: beam splitter; SLF: spatial light filter.

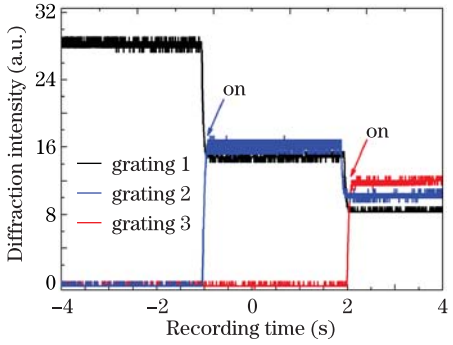

Fig. 5. (Color online) Formation process of multiplexed holography. The arrows indicate when the writing light is on.

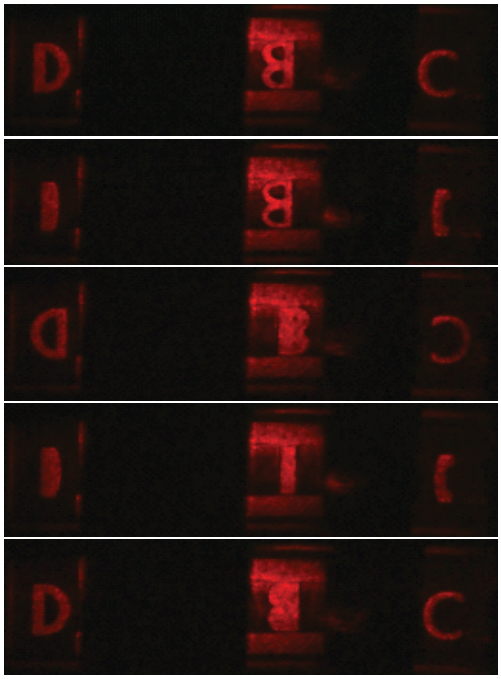

Fig. 6. (Color online) A set of snapshots taken from the real-time holographic video.

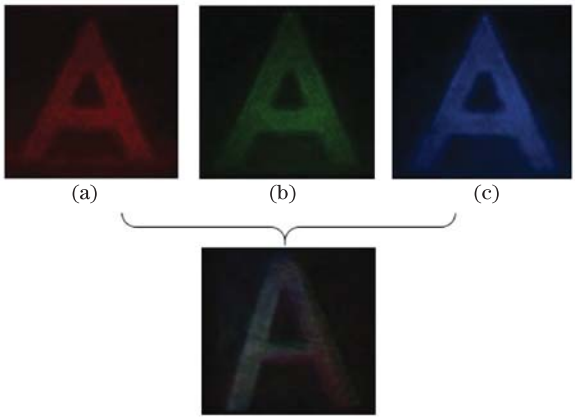

Fig. 7. (Color online) (a)−(c) Reconstructed images via He-Ne laser, Nd: YAG laser, and Sapphire laser, respectively, (d) a color holographic image by merging RGB reconstructed images.

where d is the cell thickness, $\Delta\bar{n}$ is the photoinduced refractive-index change, λ is the wavelength of reading light and M is the number of recorded gratings in the cell. The diffraction efficiency is defined as the ratio of the first-order diffraction intensity to the probe light intensity. The diffraction efficiencies of Hologram D, B and C range from 0.1 % to 0.5 %.

Figure 6 shows a set of snapshots taken from a holographic video demonstrating the revolving letters D, B, and C. As shown in Fig. 3, the response time of the cell is about 1.9 ms measured by an oscilloscope, indicating that the hologram formed in the sample is a transient hologram, thus the videos loaded by SLMs can be reconstructed at the same speed without crosstalk between frames. Furthermore, the organic photorefractive material can be easily made large size, thus it is versatile and possible to obtain large images.

A color image can be achieved by superposition of three monochromatic (red, green, and blue) reconstructed images. Therefore, we can record three holograms and reconstruct RGB images using multiplexing technique. Due to different recording conditions for RGB holograms, the three reconstructed images do not have the same size on the reconstructed image plane, which is related to the diffraction angle determined by Eq. (2)[14−15],

$$\sin\theta_m = m\frac{2n_{\rm r}\lambda_p}{n_{\rm p}\lambda_{\rm r}}\sin\theta_{\rm r} - \sin\theta_{\rm p}, \quad m = 0, 1, 2, \cdots \quad (2)$$

where θ_m is the diffraction angle of the mth-order diffracted light, $n_{\rm p,r}$ (subscripts p and r represent the probe and recording beams, respectively) are the refractive indices encountered by the beams, $\lambda_{\rm p,r}$ are the wavelengths, and $\theta_{\rm p,r}$ are the angles intersected by the beams with the grating normal. It can be seen that the imaging regions of three holograms are determined by the above parameters. According to the color holography theory, color holographic display can be realized by properly adjusting the recording-and-reading angles of each hologram and the original image size, as illustrated in Fig. 7, which demonstrates the feasibility of a real-time color holographic display with this cell.

In conclusion, a real-time multiplexed holographic video display for the study of RGB-based color holographic 3D display is achieved in a passive azo-dye-doped LC cell and holograms can be refreshed in the order of several milliseconds Our sample can be easily fabricated into a large-size screen and need no external electric field to operate. Therefore, this material has the potential of being adopted in large-size, dynamic, and color holographic 3D displays in the future.

This work was sponsored by the National "973" Program of China (No. 2013CB328804), the National Natural Science Foundation of China (No. 61307028), and the Science & Technology Commission of Shanghai Municipality (Nos. 13ZR1420000 and 11JC1405300).

References

1. P. Benzie, J. Watson, Phil Surman, I. Rakkolainen, K. Hopf, H. Urey, V. Sainov, and C. von Kopylow, IEEE Trans. Circ. Syst. Video Tech. **17,** 1647 (2007).
2. J. Jia, Y. Wang, J. Liu, X. Li, Y. Pan, Z. Sun, B. Zhang, Q. Zhao, and W. Jiang, Appl. Opt. **52,** 1404 (2013).
3. M. Salvador, J. Prauzner, K. Meerholz, J. J. Turek, K. Jeong, and D. D. Nolte, Opt. Express **17,** 11834 (2009).
4. P. Wu, S. Q. Sun, S. Baig, and M. R. Wang, Opt. Express **20,** 3091 (2012).
5. H. Gao, X. Li, Z. He, Y. Su, and T. C. Poon, Information Display **28,** 17 (2012).
6. P. A. Blanche, A. Bablumian, R. Voorakaranam, C. Christenson, W. Lin, T. Gu, D. Flores, P. Wang, W. Y. Hsieh, M. Kathaperumal, B. Rachwal, O. Siddiqui, J. Thomas, R. A. Norwood, M. Yamamoto, and N. Peyghambarian, Nature **468,** 80 (2010).
7. S. Tay, P. A. Blanche, R. Voorakaranam, A. V. Tunc, W. Lin, S. Rokutanda, T. Gu, D. Flores, P. Wang, G. Li, P. St Hilaire, J. Thomas, R. A. Norwood, M. Yamamoto, and N. Peyghambarian, Nature **451,** 694 (2008).

8. N. Tsutsumi, K. Kinashi, and W. Sakai, Materials **5,** 1477 (2012).
9. X. Li, C. Chen, H. Gao, Z. He, Y. Xiong, H. Li, W. Hu, Z. Ye, G. He, J. Lu, and Y. Su, J. Display Technol. (to be published).
10. X. Li, C. Chen, H. Gao, Z. He, W. Hu, Y. Xiong, H. Li, and Y. Su, SID Symposium Digest of Technical Papers **44,** 228 (2013).
11. Y. Xiong, Z. He, C. P. Chen, X. Li, A. Li, Z. Ye, J. Lu, G. He, and Y. Su, Opt. Commun. **296,** 41 (2013).
12. Y. Liu, J. Dong, Y. Pu, B. Chen, H. He, and H. Wang, Opt. Express **18,** 3345 (2010).
13. H. Gao, Z. Zhou, and Y. Jiang, Appl. Opt. **47,** 1437 (2008).
14. H. Gao, J. Liu, F. Gan, and B. Ma, Appl. Opt. **48,** 3014 (2009).
15. P. Yeh, *Introduction to Photorefractive Nonlinear Optics* (Wiley, 1993).